

# APPLICATION OF THE GSF-1 ALGORITHM TO THE NEAR-OPTIMAL TIMESCALE PREDICTION OF THE HYDROGEN MASER

Laurent-Guy Bernier

METAS - Swiss Federal Office of Metrology and Accreditation

Lindenweg 50, CH-3003 Bern-Wabern, Switzerland

Tel: +41-31-3234645; Fax:+41-31-3233573

E-mail: laurent-guy.bernier@metas.ch

## Abstract

*The GSF-1 timescale prediction algorithm is a simple generalization of the second difference prediction. It is close to optimal for combinations of power-law noise processes encountered in practice. By adding a drift parameter, it can be extended for use in presence of frequency drift without loss of optimality. It is applied to the timescale prediction of the hydrogen maser.*

## INTRODUCTION

The GSF-1 timescale prediction (for Generalized Structure Function prediction of order 1) is a simple generalization of the second difference prediction for which the rms prediction error is given by a simple expression of the Allan deviation, which is in fact the square root of the second structure function of the time process to be predicted. The second difference prediction and the idea of evaluating the initial frequency offset by averaging the frequency over an interval different from the prediction interval are not new. In the NBS monograph [1] published in 1974, for example, Allan and his colleagues already discuss in a review paper the second difference prediction and the necessity of averaging the frequency over a time interval much longer than the prediction interval for an optimal prediction in presence of white frequency noise. Thirty years later, however, there is still something new and useful to be said about the properties of this simple approach to timescale prediction.

The original contribution of a previous paper [2] was to discuss the optimality of the GSF-1 prediction, not in the presence of a single type of power-law noise process, but in the presence of a combination of noise processes. It was shown that it is possible to optimize the averaging interval and to minimize the rms prediction error entirely via time domain statistics, without the need for a power-law noise model of the process. It was also shown that if a power-law spectral noise model is available, then there is a simple way to compute the rms prediction error limit set by the optimal

linear prediction theory. It was verified that in practical cases, the rms prediction error yielded by the optimized GSF-1 prediction is quite close to the optimal linear prediction limit.

The present paper goes further with two original contributions. The first is the determination of the transfer function of the linear operator associated with the GSF-1 prediction error. This makes possible a theoretical discussion of the performance and behavior of the GSF-1 prediction operator in terms of the familiar power-law noise processes. The second is the introduction of a drift parameter in the GSF-1 operator, yielding the DGSF-1 prediction (GSF-1 prediction with Drift parameter). This variant of the GSF-1 prediction allows timescale prediction in the presence of a combination of noise processes and deterministic frequency drift.

The motivation behind the development of the DGSF-1 algorithm is the project to steer our newly acquired hydrogen maser in order to generate a real-time local realization of UTC. A similar Italian project is reported in [3]. Since the clock data of a given month are published during the next month by BIPM in *Circular T*, it is necessary, as part of the steering algorithm, to perform a prediction of the maser timescale over a prediction interval in the range 1 to 2 months in order to estimate the time error at the epoch of the steering and to compute a steering correction that, on average, will cancel out the time error at the epoch of the next steering.

Another potential application of the GSF-1 and DGSF-1 algorithms is in the field of the real-time prediction of the spaceborne clocks used in global navigation satellites systems. Many of the recent publications in this field are related in one way or another to the GSF-1 prediction [4,5,6].

## DEFINITION OF THE GSF-1 PREDICTION OPERATOR

We take the usual convention that  $x(t)$ , the time process of the difference between two timescales, is the integral of the normalized frequency process  $y(t)$ ,

$$x(t) = \int_{-\infty}^t y(u)du. \quad (1)$$

We define the causal first increment operator as

$$\Delta(\tau) \{x(t)\} = x(t) - x(t - \tau), \quad (2)$$

and the causal moving average operator as

$$y(t, \tau) = \frac{1}{\tau} \int_{t-\tau}^t y(u)du. \quad (3)$$

The GSF-1 prediction was introduced and discussed extensively in [2]. The GSF-1 prediction operator can be defined as

$$\hat{x}(t + \tau_1) = x(t) + \tau_1 y(t, \tau_2). \quad (4)$$

Intuitively, the GSF-1 prediction  $\hat{x}(t + \tau_1)$  is very simple. The present value  $x(t)$  is extrapolated

into the future over a prediction interval  $\tau_1$  using the causal moving average of the frequency over averaging interval  $\tau_2$  as an estimation of the present frequency offset. The error on the prediction is given by

$$\epsilon(t, \tau_1, \tau_2) = x(t + \tau_1) - \hat{x}(t + \tau_1) = \Delta(\tau_1) \{x(t + \tau_1)\} - \frac{\tau_1}{\tau_2} \Delta(\tau_2) \{x(t)\}. \quad (5)$$

The GSF-1 prediction can be seen as a simple generalization of the basic second difference prediction discussed in [1, 8, 7, 2]. If we take an averaging interval identical to the prediction interval

$$\tau_2 = \tau_1 = \tau \quad (6)$$

then the prediction error (5) simplifies to the second difference of  $x(t)$

$$\epsilon(t, \tau) = \Delta^{(2)}(\tau) \{x(t + \tau)\} \quad (7)$$

while the rms prediction error becomes the square root of the second structure function of  $x(t)$ , which is a simple function of the Allan deviation

$$\text{rms} \{\epsilon(t, \tau)\} = \sqrt{2}\tau\sigma_y(\tau). \quad (8)$$

## OPTIMAL LINEAR PREDICTION

The theory of optimal prediction [9,8,2] says that if the noise shaping filter, used to generate a given process  $x(t)$  from white noise, is initialized not at epoch  $-\infty$ , but at epoch  $t$ , i.e. at the beginning of the prediction interval, then the output is not the process itself, but the error on the optimal prediction of the process. This property is used by Tavella and Gotta [4] for the computation of the rms value of the optimal prediction error for pure power-law noise processes, using a fractional integrator as the noise shaping filter [8]. Now if we assume that the timescale difference process  $x(t)$  can be modelled as the sum of three independent power-law noise processes, with the one-sided Power Spectral Density (PSD)  $S_{yy}(f)$  of the associated frequency process  $y(t)$  given by a RWFM (Random Walk Frequency) term  $h_{-2}$ , a FFM (Flicker Frequency) term  $h_{-1}$  and a WFM (White Frequency) term  $h_0$ ,

$$S_{yy}(f) = h_{-2}f^{-2} + h_{-1}f^{-1} + h_0f^0 \quad (9)$$

then one can determine the rms OLPE (Optimal Linear Prediction Error)  $\epsilon_0(t, \tau)$  over a prediction interval  $\tau$  by taking the rms sum of the three prediction error terms computed in [4]

$$\text{rms} \{\epsilon_o(t, \tau)\} = \sqrt{\frac{(2\pi)^2 h_{-2}}{6} \tau^3 + 2h_{-1}\tau^2 + \frac{h_0\tau}{2}}. \quad (10)$$

It is possible, using (10), to determine the OLPE without knowing how to build the optimal linear prediction operator in practice. The OLPE constitutes the true optimum, the lowest rms prediction error that a linear prediction operator can reach. We will use it as a benchmark against which the

performance of the GSF-1 and DGSF-1 operators will be compared.

## PROPERTIES OF THE GSF-1 PREDICTION

The rms value of the GSF-1 prediction error (5) can be estimated as a time domain statistic using samples of the time process  $x(t)$  recorded at a regular sampling rate, in the same way as one would proceed for estimating the Allan deviation. In [2], it is shown that for a given prediction interval  $\tau_1$ , it is possible to optimize the averaging interval  $\tau_2$ . In the practical cases discussed involving cesium clocks, it is shown that the optimized GSF-1 prediction can actually reach the OLPE limit in the case of a short-term prediction dominated by WFM noise and is typically about 15% above the OLPE limit in the case of a long-term prediction dominated by FFM noise.

If a power-law model of the time process is available, then it is possible to compute the rms GSF-1 error in the spectral domain. The rms prediction error is given by

$$\text{rms} \{ \epsilon(t, \tau_1, \tau_2) \} = \sqrt{\int_0^\infty S_{xx}(f) \times |H(j2\pi f)|^2 df} \quad (11)$$

where  $S_{xx}(f)$  is the PSD of the time process  $x(t)$  and where the transfer function  $|H(j2\pi f)|^2$  of the linear operator associated with the GSF-1 prediction error (5) is given by

$$4 \left( \frac{\tau_1}{\tau_2} \right) \left( 1 + \frac{\tau_1}{\tau_2} \right) \sin^2(\pi f \tau_2) + 4 \left( 1 + \frac{\tau_1}{\tau_2} \right) \sin^2(\pi f \tau_1) - 4 \left( \frac{\tau_1}{\tau_2} \right) \sin^2(\pi f (\tau_1 + \tau_2)). \quad (12)$$

In the special case  $\tau_2 = \tau_1 = \tau$ , the transfer function reduces to

$$16 \sin^4(\pi f \tau) \quad (13)$$

which is the transfer function of the linear operator associated with the prediction error of the second increment prediction.

We take the example of the prediction of the timescale difference TAI-TA(CH) over a prediction interval of 60 d. The noise model of TAI-TA(CH) that best fits the time domain statistic is given by  $h_0 = 8.5 \times 10^{-23}$  Hz $^{-1}$ ,  $h_{-1} = 2.4 \times 10^{-29}$  and  $h_{-2} = 2.3 \times 10^{-36}$  Hz. The computation of the rms prediction error in the spectral domain, using the above PSD model and the transfer function (12), as a function of the averaging interval  $\tau_2$  for a fixed prediction interval  $\tau_1 = 60$  d is shown in Figure 1 (solid curve). On the same figure (curve with data squares), the result reported previously in [2] and obtained by averaging the rms prediction error (5) directly in the time domain is also included. The discrepancy between the time domain result and the frequency domain result arises from the fact that the power-law spectral model does not fit perfectly the actual statistical properties of the random process. Nevertheless, both results show that the prediction error can be indeed minimized by optimizing the averaging interval  $\tau_2$  and that the optimized rms GSF-1 prediction error is actually smaller than the prediction error associated with the second difference

prediction (special case  $\tau_2 = \tau_1$  i.e. last point on the curve), given by the Allan deviation via equation (8). The optimized GSF-1 prediction yields a minimum rms prediction error of 74 ns for an optimum averaging interval  $\tau_2$  of 30 d. The OLPE obtained from (10) yields 64 ns which implies that the optimized GSF-1 prediction error is only 15% larger than the OLPE limit. It is interesting to observe that in this example the optimum averaging interval is shorter than the prediction interval and not longer. This happens when RWFM is present.

## DGSF-1 PREDICTION IN PRESENCE OF FREQUENCY DRIFT

The GSF-1 prediction does not behave well in the presence of a frequency drift because it tries to perform a prediction by estimating and extrapolating a constant initial frequency offset. We propose here to extend the capabilities of the GSF-1 prediction by introducing a deterministic drift parameter  $d$  in the prediction operator such as to remove the parabolic deterministic component of  $x(t)$ . The DGSF-1 prediction operator is defined as

$$\hat{x}(t + \tau_1) = x(t) + \tau_1 y(t, \tau_2) + \frac{1}{2} d\tau_1^2 \left(1 + \frac{\tau_2}{\tau_1}\right). \quad (14)$$

The action of this new prediction operator is equivalent to separate the time process  $x(t)$  into a deterministic part and a random part. The deterministic part is predicted using initial conditions and the drift parameter  $d$ , while the random part is predicted by applying the GSF-1 prediction operator to the drift removed random residual. In practice, the rms prediction error is averaged in the time domain for a fixed prediction interval  $\tau_1$  using all the available data recorded in the past. The first step is then to minimize the rms prediction error by adjusting the drift parameter  $d$ . This yields the optimum drift. The second step is to minimize the rms error by adjusting the averaging interval parameter  $\tau_2$ . This yields the optimum averaging interval. There is very little interaction between the two parameters. Therefore, only one or two iterations are necessary to find the optimum values. Note that the new prediction operator is identical to the original if  $d = 0$ .

In order to evaluate the DGSF-1 prediction algorithm with real data relevant to our application that is the prediction of the time scale generated by a hydrogen maser, we needed real maser data recorded over a long observation period with a stable frequency drift. It was not possible to use the data from our own hydrogen maser, which was put into service only during the spring of 2003. This is why we use the data from a NIST hydrogen maser (ID 1400201) taken from the BIPM data base where all the clocks contributing to TAI are recorded. The recording of the difference UTC-CLOCK in ns shows that during 825 days (165 data points), from MJD 51299 to MJD 52124, the drift of this hydrogen maser was approximately constant at a rate of 0.012 ns/d<sup>2</sup>, which is equivalent to  $1.4 \times 10^{-16}$  1/d. The 5 d average rate of UTC-CLOCK in ns/d recorded during this period is shown in Figure 2.

The optimization of the drift parameter  $d$  in the time domain using (14) is shown in Figure 3. The

optimum drift parameter obtained is  $0.0116 \text{ ns/d}^2$ . The optimization of the averaging interval  $\tau_2$  in the time domain is shown on Figure 4 (curve with data squares). The optimum averaging interval is 50 d. For small values of  $\tau_2$ , the rms error goes down because the noise is dominated by WFM. For large values of  $\tau_2$ , the curve flattens out because the long-term is dominated by FFM. This time domain computation is to be compared with the spectral domain computation in the same figure (solid curve), which was obtained by applying the GSF-1 transfer function to the spectral model of the drift removed residual. The Allan deviation of the drift-removed residual is reported in Figure 5. The power-law spectral model of the residual is  $h_{-1} = 1.8 \times 10^{-30}$  and  $h_0 = 9.25 \times 10^{-30} \text{ Hz}^{-1}$ . There is also a WPM (White Phase) noise component in the residual that is a quantization noise due to the fact that the BIPM clock data are rounded to the nearest ns. The WPM contributes to 1 ns in the prediction error budget and is negligible in a long-term prediction. The slight discrepancy between the curves of Figure 4 comes from the fact that the power-law model of the drift-removed residual does not perfectly match the actual statistical properties of the residual. Nevertheless, the curve obtained in the spectral domain via the power-law model confirms the hypothesis that the behavior of the rms prediction error vs.  $\tau_2$  curve computed in the time domain is well described by a combination of WFM and FFM in the residual. The optimized DGSF-1 rms prediction error obtained is 12.6 ns for a prediction interval of 60 d. The OLPE limit can be estimated using (10) and the power-law model of the residual yielding 10 ns. This implies that the DGSF-1 prediction yields a rms prediction error 25% larger than the OLPE limit. The DGSF-1 prediction error process is shown on Figure 6. The process represents the individual prediction errors obtained by applying the prediction operator to each epoch  $t$  in the recorded past data. The prediction error process seems to be quite stationary, which indicates a constant frequency drift, except at the end of the recording, which shows larger deviations.

## APPLICATION TO THE METAS HYDROGEN MASER

The timescale data recorded up to now from the newly acquired METAS hydrogen maser (BIPM ID 1405701) are shown on Figure 7. There are only 29 data points (145 days of operation). Nevertheless, we have performed a DGSF-1 time domain analysis on the available data. The optimum drift parameter obtained is  $-0.071 \text{ ns/d}^2$ . The optimum averaging interval is 35 d and the DGSF-1 optimum rms prediction error is only 6.5 ns for a prediction interval of 60 d. This result is probably optimistic due to the limited data available. However, it seems to indicate that the drift is quite stable. We are looking forward to accumulate more statistics and to test in the near future a steering algorithm based on the DGSF-1 prediction.

## CONCLUSION

In this paper, we have introduced the DGSF-1 prediction algorithm, a simple generalization of the GSF-1 algorithm usable in the presence of frequency drift. Although the DGSF-1 algorithm is simple to implement in the time domain and does not require a power-law spectral model of the

time process to be predicted, it yields, after optimization of the drift parameter and of the averaging interval, a rms prediction error which is close to the OLPE theoretical limit set by the optimal linear prediction theory. Moreover, the DGSF-1 prediction algorithm was evaluated using real hydrogen maser data published by the BIPM. In the case of a typical hydrogen maser for which the drift-removed residual is dominated by white frequency and flicker frequency noise processes, a rms prediction error of 13 ns was obtained for a prediction interval  $\tau_1 = 60$  d. This rms prediction error is only 25% larger than the OLPE limit computed via the spectral model of the residual.

We have also introduced the transfer function of the linear operator associated with the GSF-1 prediction. This transfer function allows the spectral computation of the theoretical GSF-1 rms prediction error when a power-law model of the time process to be predicted is available.

In the future, we plan to apply the DGSF-1 algorithm to the steering of our own hydrogen maser in order to generate an accurate and stable realization of UTC to be used in the METAS Time & Frequency Laboratory.

- [1] D. W. Allan, J. E. Gray, and H. E. Machlan, 1974, “*The National Bureau of Standards Atomic Time Scale: Generation, Stability, Accuracy and Accessibility*,” in **National Bureau of Standards Monograph 140, Time and Frequency: Theory and Fundamentals**, pp. 205–231.
- [2] L. G. Bernier, 2003, “*Use of the Allan Deviation and Linear Prediction for the Determination of the Uncertainty on Time Calibrations Against Predicted Timescales*,” in **IEEE Transactions on Instrumentation and Measurement**, IM-52, 483–486.
- [3] G. Panfilo and P. Tavella, 2003, “*Preliminary Test on the Steering Algorithm for Keeping a Time Scale Synchronized to UTC*,” in Proceedings of the 2003 IEEE International Frequency Control Symposium & PDA Exhibition Jointly with the 17th European Frequency and Time Forum (EFTF), 5-8 May 2003, Tampa, Florida, USA (IEEE Publication 03CH37409C), pp. 301–305.
- [4] P. Tavella and M. Gotta, 2000, “*Uncertainty and Prediction of Clock Errors in Space and Ground Applications*,” in Proceedings of the 14th European Frequency and Time Forum (EFTF), 14-16 March 2000, Torino, Italy (Istituto Elettrotecnico Nazionale Galileo Ferraris, Torino), pp. 77–81.
- [5] J. Delporte, F. Vernotte, T. Tournier, and M. Brunet, 2001, “*Modelisation and Extrapolation of Time Deviation: Application to the Estimation of the Datation Stability of a Navigation Payload*,” in Proceedings of the 15th European Frequency and Time Forum (EFTF), 6-8 March 2001, Neuchâtel, Switzerland (Swiss Foundation for Research in Microtechnology, Neuchâtel), pp. 245–249.
- [6] G. Busca and Q. Wang, 2003, “*Time Prediction Accuracy for Space Clock*,” **Metrologia**, 40, S265–S269.

- [7] A. Lepek, 1997, “*Clock Prediction and Characterization*,” **Metrologia**, **34**, 379–386.
- [8] L. G. Bernier, 1988, “*Linear Prediction of the Non-Stationary Clock Error Function*,” in Proceedings of the European Frequency and Time Forum (EFTF), 16-18 March 1988, Neuchâtel, Switzerland (Neuchâtel University), pp. 125–137.
- [9] J. Makhoul, 1975, “*Linear Prediction: A Tutorial Review*,” in **Proceedings of the IEEE**, **63**, no. 4.

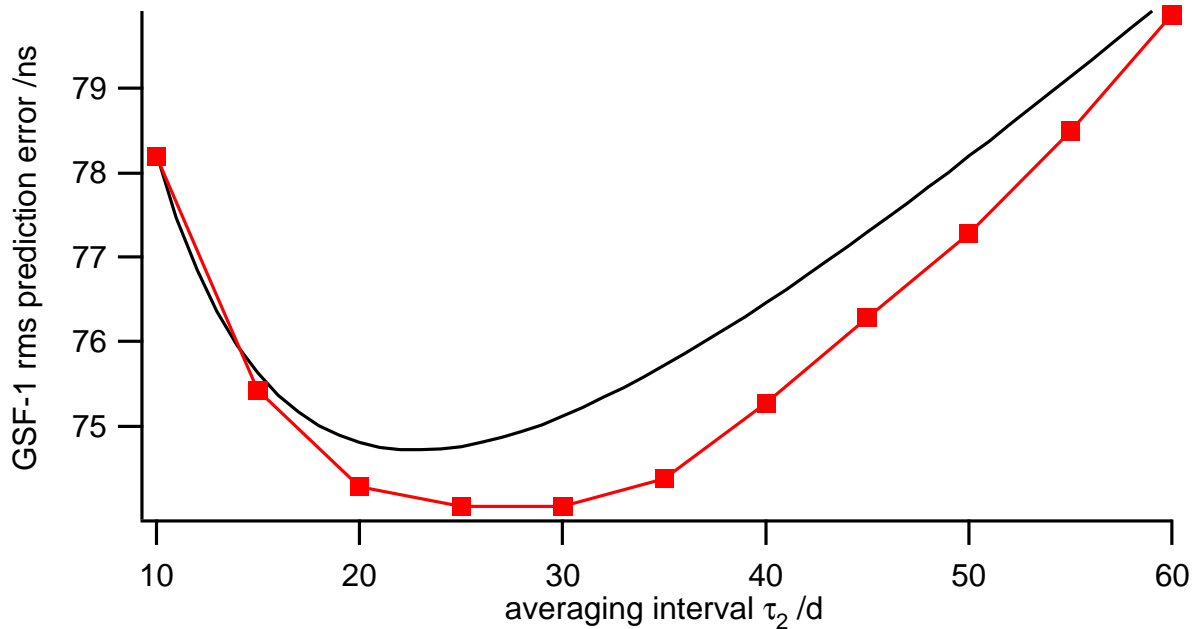


Figure 1: (curve with data squares) Rms value of the GSF-1 prediction error computed in the time domain for TAI - TA (CH) as a function of the averaging interval  $\tau_2$  for a fixed prediction interval  $\tau_1 = 60$  d. (smooth curve) Rms value computed in the spectral domain using the transfer function (12) and the PSD model given in the text.

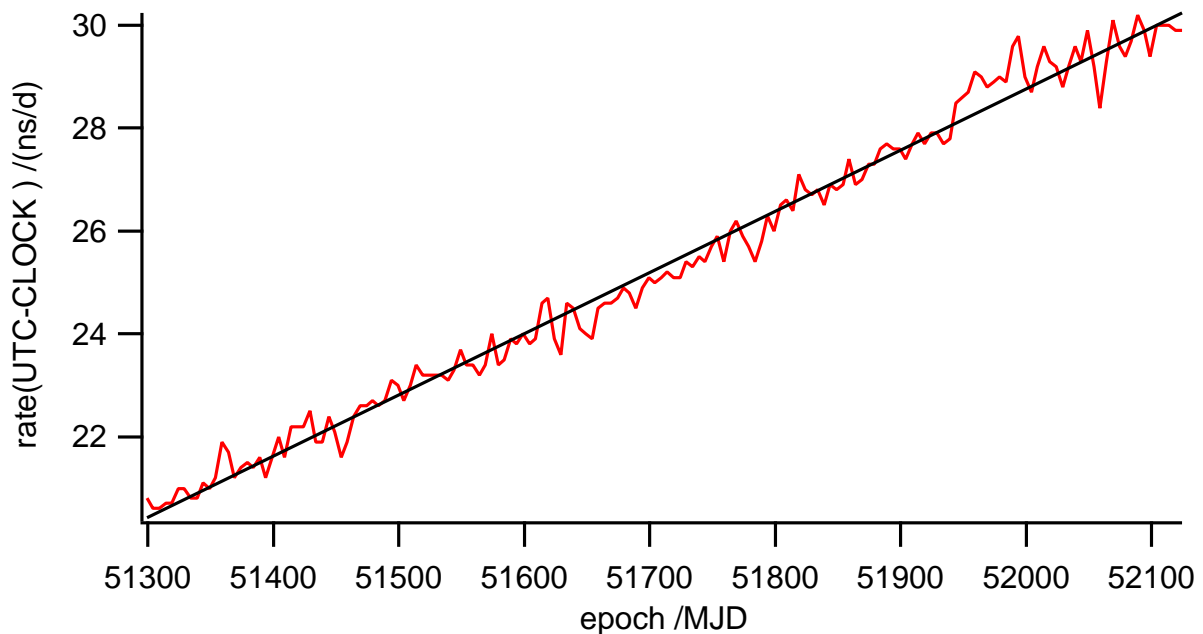


Figure 2: Five-day average rate of UTC - CLOCK in ns/d as a function of the epoch in MJD for NIST hydrogen maser ID 1400201 as downloaded from the BIPM database. The recording covers a period of 825 d (165 data points) during which the frequency drift was stable at a level of  $+0.012 \text{ ns/d}^2$ .

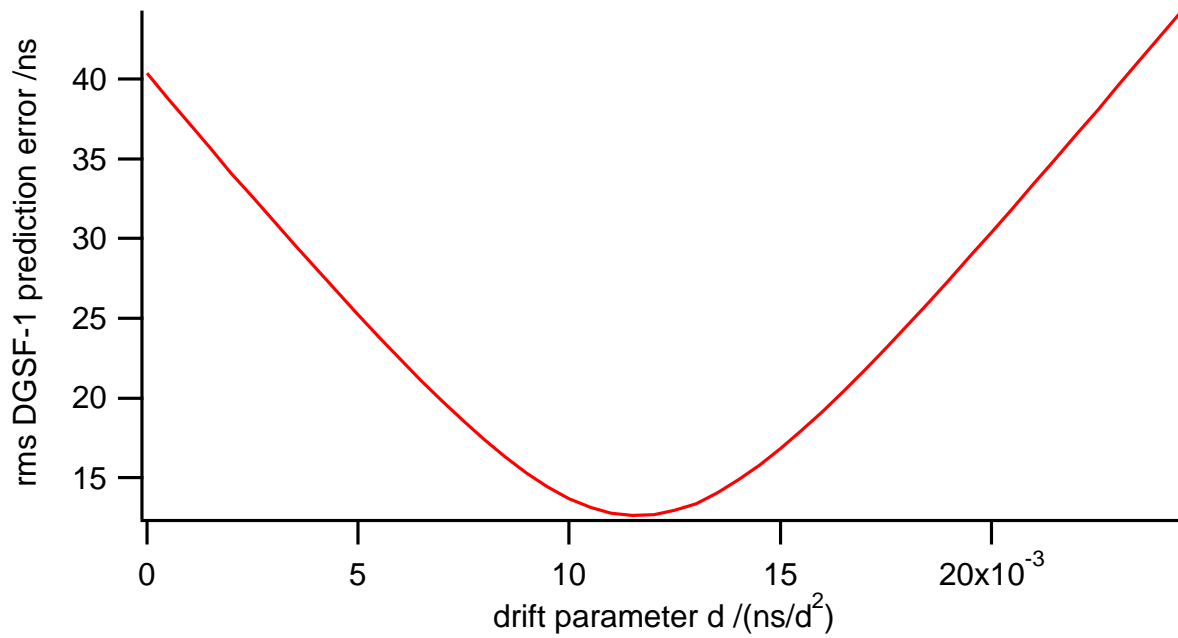


Figure 3: Optimization of the rms DGSF-1 prediction error computed in the time domain from (14) as a function of the drift parameter  $d$ , for a fixed prediction interval  $\tau_1 = 60$  d and fixed averaging interval  $\tau_2$ , and applied to the NIST hydrogen maser ID 1400201 time domain data.

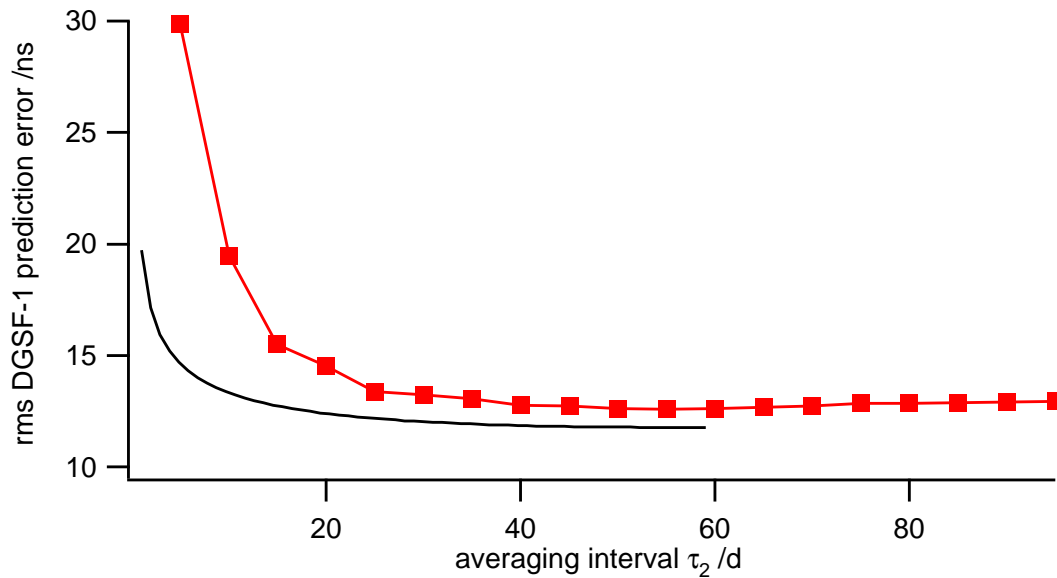


Figure 4: (curve with squares) Optimization of the rms DGSF-1 prediction error computed in the time domain from (14) as a function of the averaging interval parameter  $\tau_2$ , for a fixed prediction interval  $\tau_1 = 60$  d and fixed drift parameter  $d$ , and applied to the NIST hydrogen maser ID 1400201 time domain data. (smooth curve) RMS DGSF-1 prediction error computed in the spectral domain using the power-law model of the drift-removed residual as defined in the text.

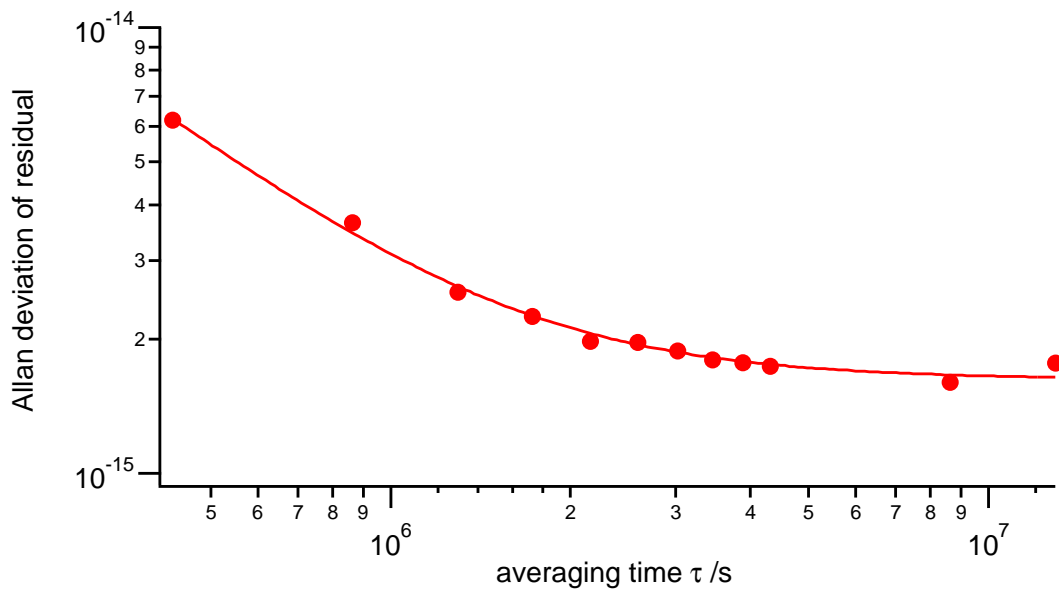


Figure 5: Allan deviation of the drift-removed residual of NIST hydrogen maser ID 1400201. The corresponding power-law spectral model is given in the text.

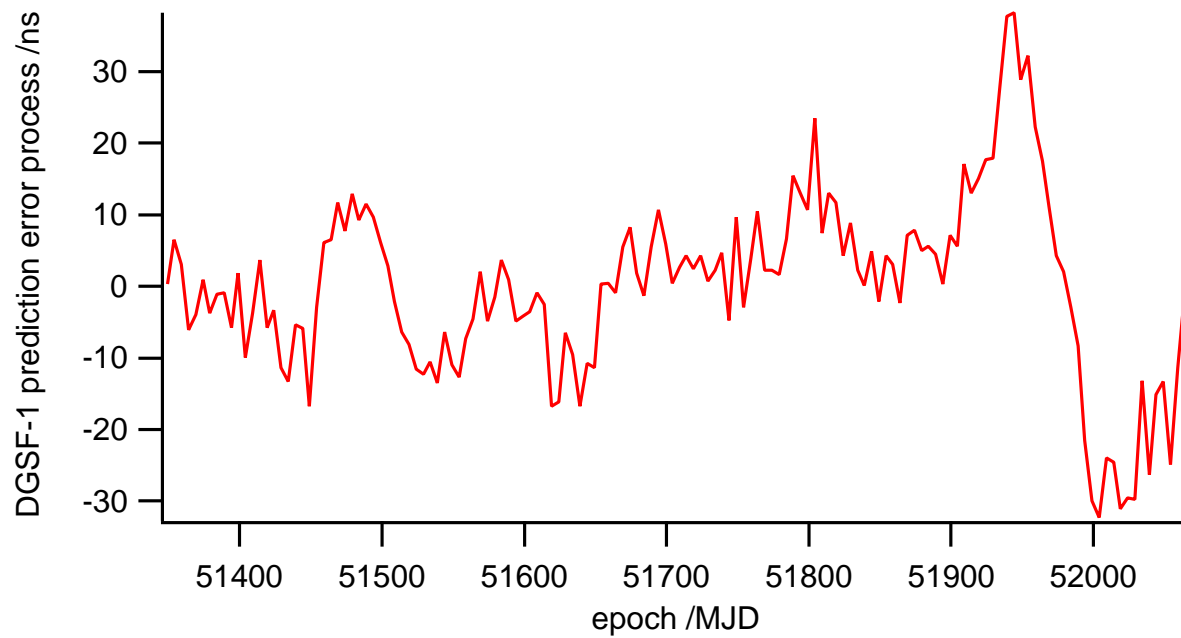


Figure 6: DGSF-1 prediction error process as a function of the present epoch in MJD computed from (14) with the optimum parameters  $d = +0.0116 \text{ ns/d}^2$  and  $\tau_2 = 50 \text{ d}$ , and applied to the NIST hydrogen maser ID 1400201 time domain data.

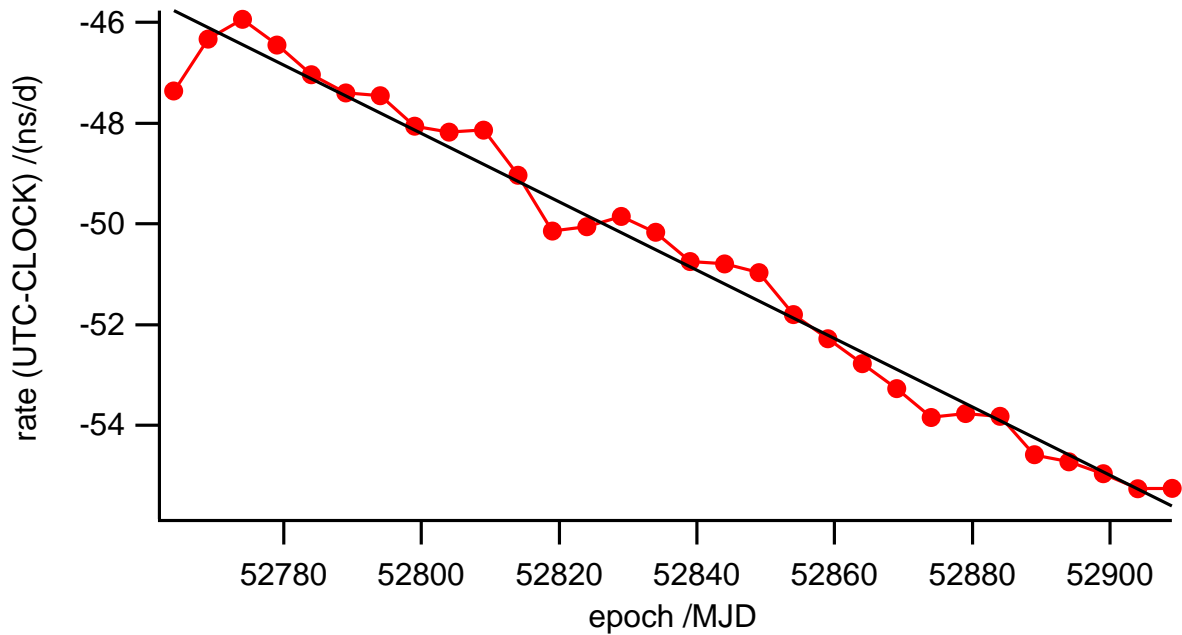


Figure 7: Five-day average rate of UTC - CLOCK in ns/d as a function of the epoch in MJD for METAS hydrogen maser ID 1405701 as downloaded from the BIPM database. The recording covers a period of 145 d (29 data points), during which the frequency drift was stable at a level of  $-0.068 \text{ ns/d}^2$ .

## **QUESTIONS AND ANSWERS**

**DAVE HOWE (National Institute of Standards and Technology):** Just a comment. Suppose you have a change in the drift or a fairly radical change in frequency, for some reason. I would like to know what your feeling is regarding the  $T_2$  and  $T_1$  ratio in that case. How that affects the ratio in the optimum prediction that you devised?

The second question is, was there an error in your drift coefficient, because it looked like you are multiplying  $1+T_2/T_1$ . That would mean if the taus are the same, then with those T values, you would have one plus one, which is two. So maybe I missed something there.

**LAURENT-GUY BERNIER:** For the first thing, of course if there is an accident, if there is a big change in the drift, of course it does not work very well. So in addition to the prediction in the presence of noise, you have to implement some scheme to detect steps in the rate of change of frequency.

But, for the second question, can you please repeat that?

**HOWE:** You had the equation in drift coefficient times tau squared. All right, it is  $1+T_2/T_1$ . Ordinarily  $T_2$  and  $T_1$  are equal. They are equal in that polynomial; you get one plus one, which is two.

**BERNIER:** Yes, if you put  $T_1$  equal to  $T_2$ , you go back to the original second-difference prediction. Then, in this case, it is a little more complicated, because you have to remove the deterministic effect during this period before the prediction to remove the initial frequency offset. There is another component that removes the deterministic component during the prediction interval.